

# IMPROVEMENT ON EDGE DROP IN COLD ROLLING OF SILICON STEEL

S. Y. Han\*, J.T. Kim\*, Y.H. Lee\* and J.J. Yi\*

(Received March 22, 1991)

Since silicon steel is used in a laminated form, thickness profile in the width and the rolling directions should be accurately controlled. It is well known that the phenomenon of edge drop is one of very serious problems in cold rolling of silicon steel. In order to determine one of the better methods for reducing edge drop, a computer simulation was carried out in this study under various rolling conditions. It was found that the better way to reduce edge drop was to use a tapered work roll. A table was given for the optimal taper crown depending upon the diameter of work roll and the width of strip. The optimal condition was applied for actual cold rolling of silicon steel. As a result, edge drop was significantly alleviated.

**Key Words:** Edge Drop, Tapered Work Roll, Thermal Crown, Thickness Profile

## NOMENCLATURE

$A_{ij}$  : Influence coefficient due to bending [Fig. 5]  
 $B$  : Width of strip [Fig. 12]  
 $c$  : Friction coefficient between WR (work roll) and BUR (back-up roll)  
 $D_{ij}$  : Flattening at center of the  $i$ th element when unit load is applied at center of the  $j$ th element [equation (13), Fig. 5]  
 $d(i)$  : Flattening between WR and strip at the  $i$ th element [Eq. (12)]  
 $E$  : Young's modulus of roll  
 $E_w$  : Young's modulus of WR [Eq. (13)]  
 $i, j$  : Element index [Fig. 4]  
 $K_s$  : Spring constant between WR and BUR [equation (11)]  
 $L_{bw}$  : Relative rigid displacement between WR and BUR [Eq. (5)]  
 $ld$  : Contact length between WR and strip [Eq. (13)]  
 $N$  : Number of elements [Fig. 4]  
 $P_i$  : Rolling force between WR and strip at the  $i$ th element [Eq. (1), Fig. 4]  
 $Q_i$  : Contact pressure between WR and BUR at the  $i$ th element [Eq. (1), Fig. 4]  
 $P_b$  : Reaction force in the  $y$ -direction at BUR bearing [Eq. (3), Fig. 4]  
 $R_b$  : Reaction force in the  $z$ -direction at BUR bearing [Eq. (4), Fig. 4]  
 $R_{cb}$  : Crown of BUR [Eq. (11)]  
 $R_{cw}$  : Crown of WR [Eq. (11)]  
 $S_i$  : Contact pressure between WR and IMR of SRB (support roller bearing) at the  $i$ th element [equation (1), Fig. 4]  
 $Y_{by}$  : Deformation of BUR in the  $y$ -direction [Eq. (7)]  
 $Y_{bz}$  : Deformation of BUR in the  $z$ -direction [Eq. (8)]  
 $Y_{ws}$  : Displacement at contact point between WR and strip

$Y_{wy}$  : Deformation of WR in the  $y$ -direction [Eq. (5)]  
 $Y_{wz}$  : Deformation of WR in the  $z$ -direction [Eq. (5)]  
 $Y_{ba}(i)$  : Displacement of BUR in the  $\theta_i$ -direction [Eq. (10)]  
 $Y_{wa}(i)$  : Displacement of WR in the  $\theta_i$ -direction [Eq. (9)]  
 $\theta_i$  : The applied angle of contact pressure  $Q_i$  [Eq. (1), Fig. 4]  
 $\beta_i$  : The applied angle of contact pressure  $S_i$  [Eq. (1), Fig. 4]  
 $\nu$  : Poisson's ratio [Eq. (11)]  
 $\Delta x$  : Length increment in the  $x$ -direction

## 1. INTRODUCTION

Since silicon steel is used for elements of electric and electronic products in a laminated form, strip thickness profile should be controlled rigorously in the width direction as well as in the rolling direction. Since the accuracy of strip dimension and flatness for cold rolling sheet is strictly required, many studies have been made so far. For strip thickness profile in the rolling direction, techniques of automatic gauge control (Waker and Cook, 1958) and automatic tension limit control (ISIJ, 1983) have been used. For strip thickness profile in the width direction, automatic shape control system (Yasuda, 1987) and various types of mills such as conventional 6-hi and CVC (Continuously Variable Crown) mills, which have an excellent capability of strip crown control [McDonald and Spooner, 1987], have been developed and applied at actual plants.

At present, MKW (Mehrwalzen Kalt Walzwerk) mill, which has the characteristics of 4-hi mill and sendzimir mill, has been used for domestic cold rolling of silicon steel. Although problems in strip thickness profile in the rolling direction were not serious through the improvement of equipment, thickness deviation in the width direction, namely, edge drop was one of very serious problems. Very severe edge drop was occurred especially on M-class of non-oriented grain silicon steel, and it was a main cause of reducing productivity and actual yield.

\*Department of Steel Product, Research Institute of Industrial Science and Technology, P.O. Box 135, Pohang 790-600, Korea

Therefore, we have carried out a computer simulation in order to find one of the better methods to reduce edge drop for M-class silicon steel throughout the elastic deformation analysis of rolls and the measurements of deformation resistance and thermal crown. Then the effect of the better method we had found was verified by applying it to an actual plant.

## 2. METHOD OF SOLUTION

### 2.1 MKW Mill

Due to the effect of Si in silicon steel, the varying region of deformation resistance becomes wider and its absolute value is also larger compared with those of mild steel as cold rolling goes on. Thus, the conventional cold rolling of silicon steel has some difficulties in flatness control at exit as well as in rolling work by the large variation of rolling force according to rolling conditions.

In order to remedy these difficulties, MKW mill has been used for cold rolling of silicon steel. The schematic diagram of MKW mill is shown in Fig. 1 and the characteristics of MKW mill are as follows;

- (1) reversing mill combining the characteristics of 4-hi and sendzimir mills
- (2) rolling capability of high strength material by small diameter of WR (work roll)
- (3) flatness control function by SRB (Support Roller Bearing) system
- (4) thermal crown control function by zone coolant system
- (5) BUR (back-up roll) drive, and no WR chock
- (6) eccentricity between the centers of WR and BUR in order to prevent WR from getting away

Edge drop (ISIJ, 1986) is the phenomenon of a sudden thickness reduction at strip edge and is defined by thickness deviation between thickness at strip edge and thickness at a 25mm distance from the edge. Strip crown is defined by thickness deviation between thickness at the center and thickness at a 25mm distance from strip edge. The definitions are illustrated in Fig. 2.

### 2.2 Measurements of Hot and Cold Coil Profiles

In order to use for input data of computer simulation, hot coil profile was measured by 22mm in the width direction by use of a micrometer after obtaining a specimen at exit of APL (annealing and pickling line). And cold coil profile was also measured in the same manner after obtaining a specimen at entry of CAL (continuous annealing line) in order to examine the validity of simulation program.

### 2.3 Measurement of WR Thermal Crown

WR thermal crown yielded by deformation energy of strip and friction energy between strip and work rolls was measured by roll gap measurement method. At first, Al wire of diameter 5mm was prepared and it was softened by annealing for half an hour at 480°C. As shown in Fig. 3, a measurement apparatus like a ladder was manufactured by the dimensions of width 50mm and length 2m. The thermal crown was measured by inserting the apparatus into the work roll gap in the barrel length direction.

The measurement method of WR thermal crown is as follows. Before cold rolling of M-class silicon steel began, both work rolls were exchanged. The apparatus was inserted into work roll gap, we compressed the apparatus by 2~3mm

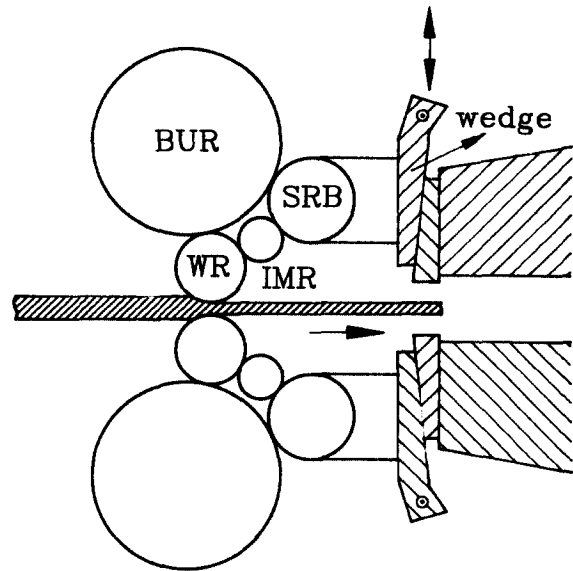
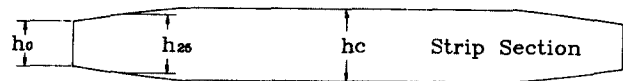


Fig. 1 The schematic diagram of MKW mill



$$\left\{ \begin{array}{l} \text{Crown : } C_{25} = h_c - h_{25} \\ \text{Edge drop : } E_{25} = h_{25} - h_0 \end{array} \right.$$

Fig. 2 The definitions of strip crown and edge drop

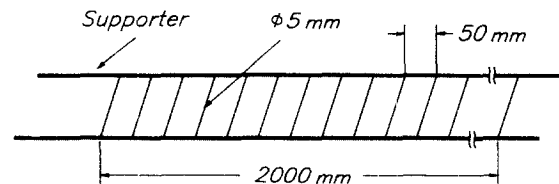


Fig. 3 Apparatus for measuring thermal crown

downward. Then initial crown was checked by measuring thickness difference along compressed traces of Al wire using a micrometer. Total work roll crown after one hot coil was rolled, was measured in the same manner. Then, thermal crown was determined by subtracting initial crown from measured total work roll crown with respect to roll edge. In this manner, thermal crowns were repeatedly measured until the work rolls were exchanged. In fact, although the effect of wear by the slip between strip and work rolls was included in the measurement, it was ignored since the wear was negligible due to the short running time of work rolls. The rolling conditions at measurement are shown in Table 1.

Table 1 Rolling conditions for measuring thermal crown

BUR Dia.	1320mm
WR Dia.	205mm
WR Initial Crown	0.10mm
Strip Width	936mm
Measuring Width	1250mm

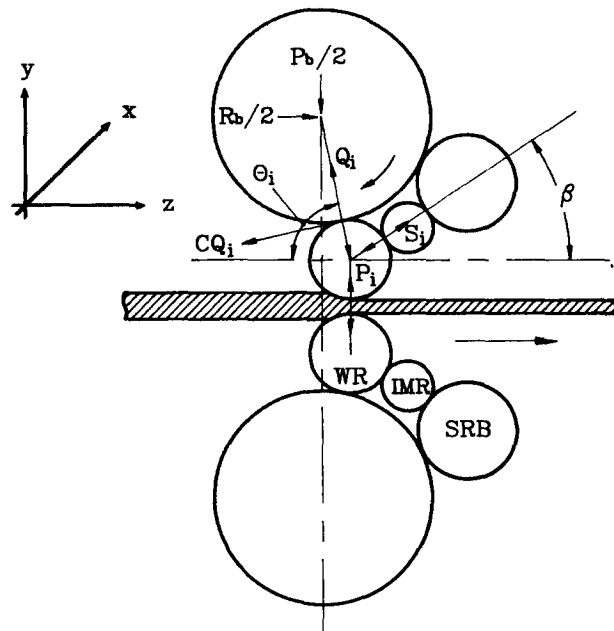
2.3 Elastic Deformation Analysis

(1) Modelling

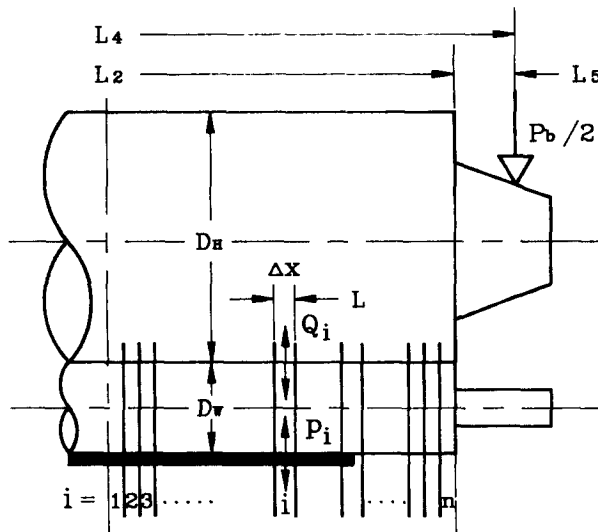
The roll constitution of MKW mill is shown in Fig. 4(a) and the division model shown in Fig. 4(b) was applied for elastic deformation analysis of rolls. The assumptions used for analysis are as follows :

- rolling is symmetric with respect to y-axis.
- displacement in the rolling direction of BUR is ignored.
- tension distribution in the width direction is constant.
- rigid displacement of WR in the z-direction is ignored.

In addition, contact pressures  $S_i$ 's from SRB system are assumed to be known since it has been reported that the effect of contact pressures  $S_i$ 's is very little on strip edge (Monda, 1984), and we are interested in finding a better method to reduce edge drop.



(a) the roll constitution



(b) the division model

Fig. 4 Analysis model of MKW mill

(A) Equilibrium equations

From Fig. 4(a), equilibrium equations are obtained as follows.

- WR

- y-direction

$$\sum_{j=1}^N P_j \Delta x - \sum_{j=1}^N S_j \sin \beta \Delta x = \sum_{j=1}^N Q_j \sin \theta_j \Delta x + c \sum_{j=1}^N Q_j \cos \theta_j \Delta x \quad (1)$$

- z-direction

$$\sum_{j=1}^N S_j \cos \beta \Delta x = -c \sum_{j=1}^N Q_j \sin \theta_j \Delta x + \sum_{j=1}^N Q_j \cos \theta_j \Delta x \quad (2)$$

- BUR

- y-direction

$$\sum_{j=1}^N Q_j \sin \theta_j \Delta x + c \sum_{j=1}^N Q_j \cos \theta_j \Delta x - P_b/2 = 0 \quad (3)$$

- z-direction

$$\sum_{j=1}^N Q_j \cos \theta_j \Delta x - c \sum_{j=1}^N Q_j \sin \theta_j \Delta x - R_b/2 = 0 \quad (4)$$

(B) Deformation of rolls

In the case of symmetric rolling, deformation of rolls can be obtained by applying the solution of deformation of simple supported beam (ISIJ, 1983) as shown in Fig. 5. The influence coefficients  $A_{ij}$ 's, which mean the deformation at the center of the  $i$ th element when unit load is applied at the center of the  $j$ th element, due to bending considering shear force can be represented by the following equations.

- (i)  $j \leq i (\eta \geq \beta)$

$$A_{ij} = \frac{32}{3E\pi} [(1+v) \left\{ \frac{L_5}{d^2} + \frac{\beta - L_5}{D^2} \right\} + \frac{2L_5^3}{d^4} + \frac{1}{D^4} (3\eta\beta L_4 - 2L_5^3 - 3\beta\eta^2 - \beta^3)]$$

- (ii)  $j > i (\eta < \beta)$

$$A_{ij} = \frac{32}{3E\pi} [(1+v) \left\{ \frac{L_5}{d^2} + \frac{\eta - L_5}{D^2} \right\} + \frac{2L_5^3}{d^4} + \frac{1}{D^4} (3\eta\beta L_4 - 2L_5^3 - 3\eta\beta^2 - \eta^3)]$$

where,

$$\eta = \frac{L_4}{2} - (j - 0.5) \Delta x$$

$$\beta = \frac{L_4}{2} - (i - 0.5) \Delta x$$

The deformations of WR and BUR can be obtained from influence coefficients  $A_{ij}$ 's due to bending considering shear forces by rolling forces  $P_j$ 's, contact pressures  $Q_j$ 's and  $S_j$ 's, and relative rigid displacement  $L_{bw}$ .

- WR

- y-direction

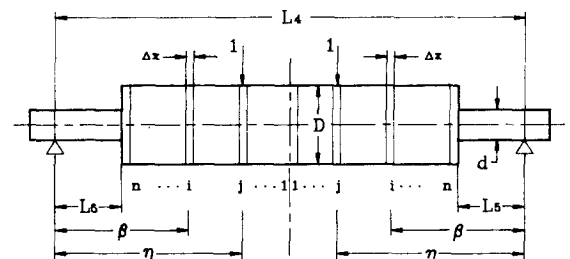


Fig. 5 Analysis model for influence coefficient  $A_{ij}$

$$Y_{wy}(i) = \sum_{j=1}^N A_{ij} P_j \Delta x - \sum_{j=1}^N A_{ij} S_j \sin \beta \Delta x + L_{bw} - \sum_{j=1}^N A_{ij} Q_j \sin \theta_j \Delta x - c \sum_{j=1}^N A_{ij} Q_j \cos \theta_j \Delta x \quad (5)$$

• z-direction

$$Y_{wz}(i) = \sum_{j=1}^N A_{ij} S_j \cos \beta \Delta x + c \sum_{j=1}^N A_{ij} Q_j \sin \theta_j \Delta x - \sum_{j=1}^N A_{ij} Q_j \cos \theta_j \Delta x \quad (6)$$

• BUR

• y-direction

$$Y_{by}(i) = \sum_{j=1}^N A_{ij} Q_j \sin \theta_j \Delta x + c \sum_{j=1}^N A_{ij} Q_j \cos \theta_j \Delta x \quad (7)$$

• z-direction

$$Y_{bz}(i) = \sum_{j=1}^N A_{ij} Q_j \cos \theta_j \Delta x - c \sum_{j=1}^N A_{ij} Q_j \sin \theta_j \Delta x \quad (8)$$

### (C) Compatibility equations

The deformations of WR and BUR with respect to the angle  $\theta_i$  between z-axis and the line from center of WR to center of BUR were obtained as follows.

$$Y_{w\theta}(i) = Y_{wz}(i) \cos \theta_i + Y_{wy}(i) \sin \theta_i \quad (9)$$

$$Y_{b\theta}(i) = Y_{bz}(i) \cos \theta_i + Y_{by}(i) \sin \theta_i \quad (10)$$

By using two equations above, the following compatibility equations were obtained.

$$Y_{b\theta}(i) - Y_{w\theta}(i) + Q(i)/K_s = -[R_{cw}(i) + R_{cb}(i)]/2 \quad (11)$$

And compatibility equations, which were used for calculating strip thickness profile at exit, at the contact points between WR and strip were obtained as follows.

$$Y_{ws}(i) = Y_{wy}(i) + d(i) - R_{cw}(i)/2 \quad (12)$$

### (D) Flattening between WR and strip

WR surface is flattened by contact pressures  $P_j$ 's between WR and strip, which directly affect the thickness profile at exit. Generally, flattening is calculated by use of the solution for elastic half-space problem based on two dimensional contact theory[Yamamoto, 1982 and Tozawa, 1970]. In the case of applying loads at two divisions, as shown in Fig. 6 flattening(Tozawa, 1970) is obtained as follows.

$$D_{ij} = \frac{1-\nu^2}{E_w} P_j [F(x'_i) + F(x''_i)] \quad (13)$$

where,

$$F(x) = \ln \frac{\sqrt{ld^2 + (x + \frac{w}{2})^2} + x + \frac{w}{2}}{\sqrt{ld^2 + (x - \frac{w}{2})^2} + x - \frac{w}{2}}$$

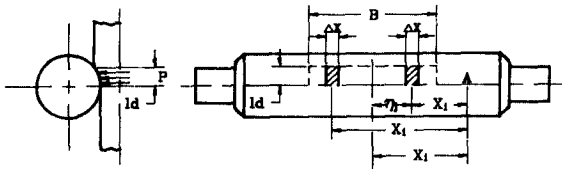


Fig. 6 Analysis model for work roll flattening

$$+ \frac{x + \frac{w}{2}}{ld} \ln \frac{\sqrt{(x + \frac{w}{2})^2 + ld^2} + ld}{x + \frac{w}{2}}$$

$$- \frac{x - \frac{w}{2}}{ld} \ln \frac{\sqrt{(x - \frac{w}{2})^2 + ld^2} + ld}{x - \frac{w}{2}}$$

where,

$$x'_i = |x_i - \eta_i|, \quad P_j = P * ld$$

$$x''_i = x_i + \eta_i, \quad w = \Delta x$$

### (2) Computer Simulation

Simulation program is prepared for calculating strip thickness profile by use of inputs of material conditions such as strip width and hot coil profile, of operation conditions such as reduction ratio and tension, and of equipment conditions such as diameters and positions of rolls. The program is composed of input, calculation of rolling force, calculation of influence coefficients, matrix composition and solver, contact condition handling, and output.

Calculation procedure is as follows. After rolling force is calculated by Brand & Ford(1948)'s equation according to target thickness at exit, the rolling forces  $P_j$ 's and the angles  $\theta_i$ 's between z-axis and the line from center of WR to center of BUR are assumed. Then after influence coefficients  $A_{ij}$ 's for WR and BUR are calculated, a matrix is composed by use of Eq. (1) and Eq. (11) in order to determine unknown contact pressures  $Q_i$ 's and relative rigid displacement  $L_{bw}$ . This matrix can be solved by Gauss Elimination method. In calculation, if some of the contact pressures  $Q_i$ 's between WR and BUR come out negative,  $Q_i$ 's and  $L_{bw}$  are recalculated by recomposing the matrix after setting the negative values to zero for those elements. For determination of  $\theta_i$ 's,  $\theta_i$ 's are recomputed from the geometric conditions considering diameters and positions of rolls, deformations of rolls, and relative rigid displacement, then iteration is carried out until the differences between assumed angles and computed angles converge to less than  $0.017(1^\circ)$  radian. From the determined contact pressures, relative rigid displacement, assumed rolling forces, flattening between WR and strip, and displacement of WR surface are obtained. After thickness profile at exit is calculated by using Eq. (12), rolling forces  $P_j$ 's are recalculated by Brand & Ford's equation. By converging the differences between previous rolling forces and calculated rolling forces to less than 100 Kg, final thickness profile at exit and the unknowns  $P_j$ 's,  $Q_i$ 's,  $\theta_i$ 's, and  $L_{bw}$  are determined.

In calculations, thickness at strip center is always maintained as target thickness at exit and strip thickness profile is calculated by relative displacements with respect to thickness at strip center. The notations of a tapered WR used for simulation are shown in Fig. 7. EL(mm) is the length of

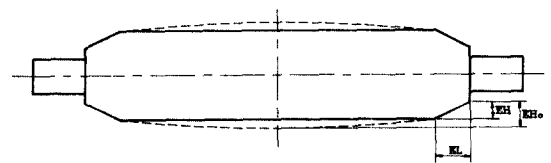
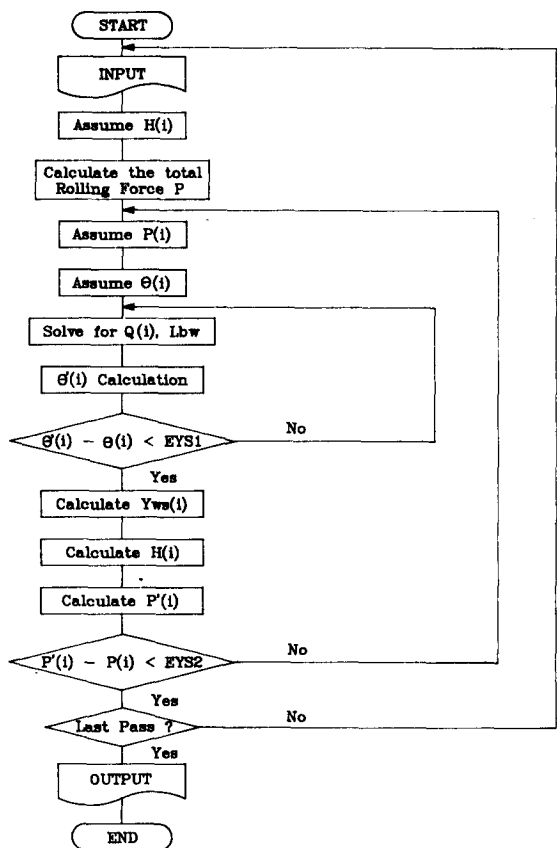


Fig. 7 Notations of tapered work roll

**Table 2** Rolling conditions for computer simulations

Mill Type	MKW Mill
Roll Barrel Length	1250mm
Back Up Roll Dia.	1320mm
Work Roll Dia.	190~230mm
Strip Width	920~1160mm
Young's Modulus	21,000kg/mm <sup>2</sup> (WR, BUR)
Poisson Ratio	0.3
Roll Initial Crown	2/100~15/100mm
Roll Taper length	100~250mm
Roll Taper height	2~250μm
Materials	M-Class
Tension	2-14kg/mm <sup>2</sup>



**Fig. 8** Flow chart for the calculation of strip profile

taper from the edge and  $EH(\mu m)$  is the height of taper corresponding to EL. Thus, in the case that both taper and parabolic initial crown are given,  $EH_c(\mu m)$ , which is the value obtained by the summation of EH to parabolic initial crown at center, practically affects the strip thickness profile. The calculation conditions are shown in Table 2 and flow chart for computer simulation is shown in Fig. 8.

### 3. RESULTS AND DISCUSSION

#### 3.1 Measurement of WR Thermal Crown

WR thermal crowns were measured after 3 passes (1.931t-1.206t - 0.781t-0.491t) rolling per one hot coil of M-class silicon steel having dimensions of thickness, 1.931mm, and width,

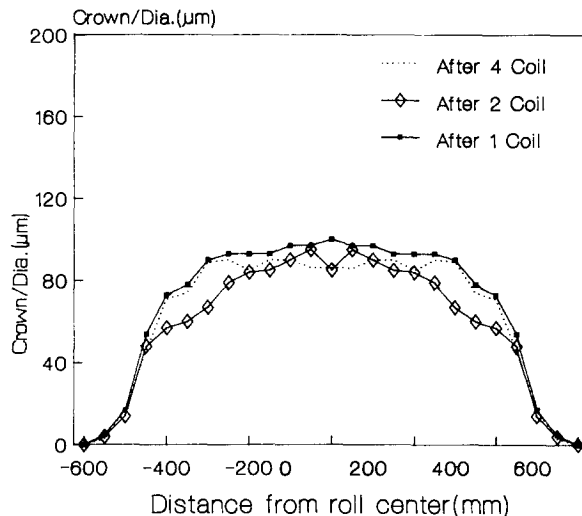


**Fig. 9** Measured thermal crown profiles of work roll (M-Class, 1.931t-0.491t, 3 pass, W : 936mm)

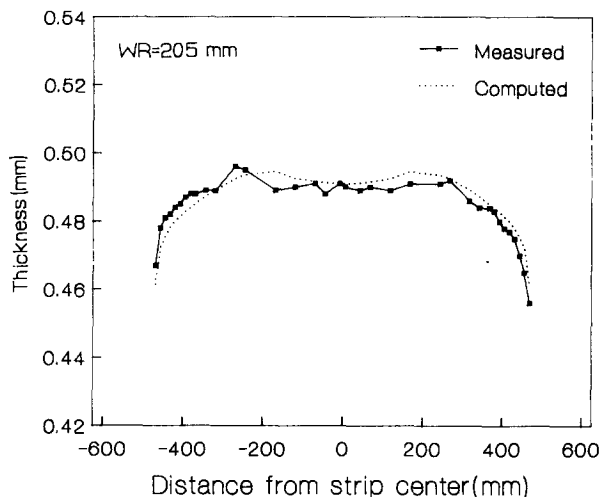


**Fig. 10** Comparison between computed and measured strip profile (M-Class, 1.931t-0.491t, 3 pass, w : 936mm)

936mm. The results are shown in Fig. 9. It was found that WR thermal crown was increased steeply at strip edge, and after one hot coil was rolled, it was almost saturated, afterwards it was maintained at almost constant magnitude. The maximum magnitude of thermal crown is almost 100μm at center, but the quantity of thermal crown affecting thickness profile is about 50 μm, which coincided with McDonald(1987)'s result.

#### 3.2 Simulation Results and Discussions

##### (1) Strip Thickness Profile

Figure 10 shows comparison between measured and computed strip thickness profiles after 3 passes rolling for M-class silicon steel having dimensions of thickness, 1.931mm, and width, 936mm by using WR diameter of 205mm. Although it shows about 5 μm differences in dimensions agreement between measured and computed profiles has been made, so that it is construed that the phenomenon of edge drop can be simulated by the program used.

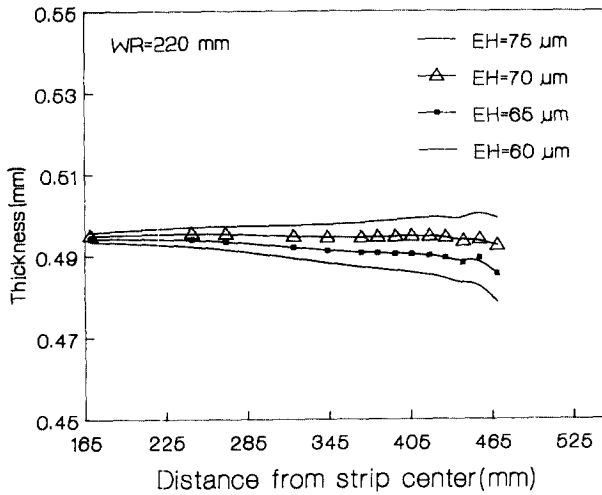


Fig. 11 Effect of the heights (EH) of tapered work roll (M-Class, 1.931t-0.491t, 3 pass, W : 936mm)

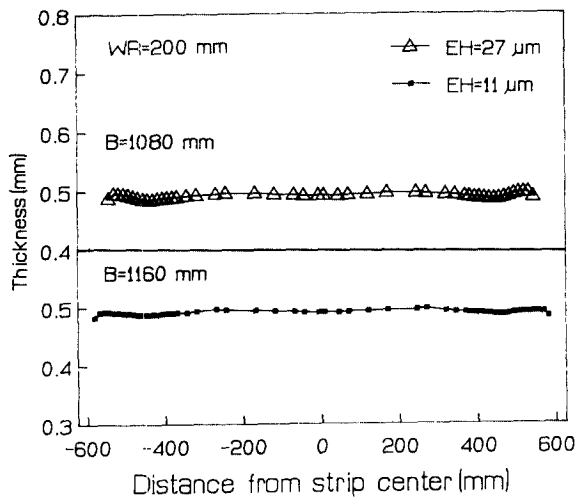


Fig. 12 The optimal EH values of tapered WR on wide strip profile (M-Class, 1.931t-0.491t, 3 pass, W : 936mm)

### (2) Effect on Edge Drop by Changing Work Roll Type

In order to derive a better way in reducing edge drop, the following 6 cases were investigated; (1) BUR with initial crown (2) BUR with only taper crown (3) BUR with both initial and taper crown (4) WR with various parabolic initial crowns (5) WR with only taper crown and (6) WR with both initial and taper crown. Among the first three cases, the method (3) was found to be the most effective but the best method was thought to be one of the last three cases by considering the fact that the exchange period and exchange time of BUR is much longer. Consequently, the best method was found to be the method (6) among the last three methods. The magnitude of initial crown was used as the currently used value in the actual plant, for instance, 0.11mm for 200mm diameter of WR.

In order to determine the optimal value of EL, many thickness profiles were calculated for various combinations of EH and EL. From those combinations, EL was chosen as 175mm considering Kitamura (1984)'s study. Next, in order to find

Table 3 The optimal values of EH according to diameters of WR (DWR) and widths of strip (EL=175mm) (unit :  $\mu\text{m}$ )

DWR	190	200	210	220	230
Width					
936	50	56	63	69	74
1080	25	27	31	34	37
1160	9	11	13	15	18

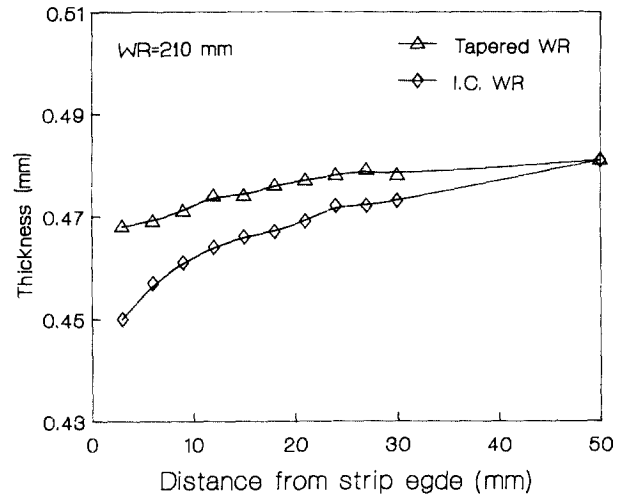


Fig. 13 The comparison of edge drop according to I.C. WR and tapered WR

the optimal value of EH, thickness profiles were calculated for various values of EH after EL was fixed by 175mm in the case of 220mm diameter of WR. Fig. 11 shows the variations of thickness profiles when EH was changed from 60  $\mu\text{m}$  to 75  $\mu\text{m}$ , where the best thickness profile was obtained in the case of EH=70  $\mu\text{m}$ . The optimal value of EH was determined by the value, which gave the best thickness profile among many thickness profiles obtained by changing EH by 1  $\mu\text{m}$  increment. In addition, the optimal values of EH were also determined by the same manner corresponding to diameters of WR's for widths of 1080 and 1160mm, those are planned to be produced in the near future. The best thickness profiles were obtained for 200mm diameter of WR when EH=27  $\mu\text{m}$  for 1080mm, and EH=11  $\mu\text{m}$  for 1160mm as shown in Fig. 12. The optimal values of EH according to diameter of WR and width of strip are shown in Table 3.

### 3.3 Application in an actual plant

The previously determined rolling parameters for reducing edge drop were applied for cold rolling of silicon steel in an actual plant. A tapered work roll having diameter of 210mm was ground by using redesigned camber plate for grinding optimal taper crown and initial crown simultaneously. In order to examine the method, six hot coils of M-class silicon steel were selected from the same lot. Then, three hot coils were rolled by a parabolic initial crown type of WR (I. C. WR) and three hot coils were rolled by a tapered work roll, respectively. Fig. 13 shows the average thickness profiles for both cases. From this result, we can see that edge drop can be reduced significantly by rolling using a tapered work roll.

#### 4. CONCLUSIONS

The following conclusions were obtained from computer simulations and cold rolling test carried out at actual plant for reducing edge drop in rolling of M-class silicon steel.

(1) Computer simulations have been successfully made for predicting edge drop in rolling of M-class silicon steel throughout elastic deformation analysis of rolls.

(2) The use of a tapered work roll was very effective in reducing edge drop.

(3) The optimal taper crowns according to diameters of WR and widths of strip have been suggested.

(4) The previously determined rolling parameters for reducing edge drop have been reconfirmed by carrying out rolling tests in an actual plant.

#### REFERENCES

Bland, D.R. and Ford, H., 1948, "The calculation of Roll Force and Torque in Cold Strip Rolling with Tensions," Proc. I. Mech. E., Vol. 158, p.174.

The Iron and Steel Institute of Japan, 1983, "Theory and Practice of Plate Rolling," pp.89~95.

The Iron and Steel Institute of Japan, 1983, "Theory and Practice of Sheet Rolling," pp.305~308.

The Iron and Steel Institute of Japan, 1986, "A Handbook of Iron and Steel (Vol. 3, Rolling Foundation Steel Plate)," p. 395.

Kitamura, K., 1977, "On the Control of Strip Profile in Hot Rolling Mill," The Spring Conference of Tetsu-To-Hagane at Tokyo, Vol. 63, pp.A107~A110.

Kitamura, K., 1984, "Improvement of Edge Drop by Use of a Tapered Work Roll for Silicon Steel," The Spring Conference of Tetsu-To-Hagane at Kawasaki, Vol. 70, pp.A60

~A63.

Kono, T., Hase, N. and Nishino, T., 1980, "Development of Mathematical Model on Crown Control in Cold Strip Rolling," Sumitomo Metal, Vol. 32, No. 3, pp.93~103.

McDonald, I.R. and Spooner, P.D., 1987, "Improvement in Shape Performance Using CVC Rolls in 4 and 6 High Mills," 4th International Steel Rolling Conference mat IRSID, E19.1~E19.8.

Monda, K., 1984, "Deformation Analysis Program of Multi-High Mill and Application to MKW Mill," The Proceedings of the 35th Japanese Joint Conference for the Technology of Plasticity at Tokyo, pp.247~252.

Shiosaki, H., 1968, "An Analysis of Roll Bending for a Four-high Mill," J. Japan Soc. Tech. Plasticity, Vol. 9, No. 88, pp.315~323.

Shohet, K.N. and Boyce, M.F., Nov. 1968, "Static Model Tests of Roll Bending Methods of Crown Control," J. Iron and Steel Institute, Vol. 206, pp.1099~1102.

Shohet, K.N. and Townsend, N.A., 1971, "Roll Bending Method of Crown Control in Four High Mills," J. Iron and Steel Institute, Vol. 190, p.769.

Tozawa, Y., 1970, "Analysis to Obtain the Pressure Distribution from the Contour of Deformed Roll," J. Jap. Soc. Tech. Plasticity, Vol. 11, No. 108, p.29.

Tozawa, Y., 1975, "Roll Deformation and Effect of Roll Crown Affecting the Pressure Distribution," J. Japan Soc. Tech. Plasticity, Vol. 16, No. 171, pp.345~351.

Walker, N.S. and Cook, J.W., 1958, "An Automatic Gage Control System for Tandem Cold Mills," Iron and Steel Engineer, pp.124~130.

Yamamoto, 1982, "Shape Control of Plate at Z-high Mill," J. Japan Soc. Tech. Plasticity, Vol. 23, No. 263, p. 1267.

Yasuda, K., Narita, K., Shida, S., Nishi, H. and Yoshimoto, K., 1987, "Rolling of Dead Flat Strip Using UC Mill with Small Diameter Work Rolls," 4th International Steel Rolling Conference at IRSID, E22.1~E22.12.